DOI: 10.61782/fa.2025.0668

FORUM ACUSTICUM EURONOISE 2025

# OPTIMIZING VOLUME PENALIZATION FOR ACOUSTIC FDTD SIMULATIONS: MODELING ERRORS AND PARAMETER SELECTION

**Yannick Schubert** **Mathias Lemke***

Computational Fluid Dynamics Group, TU Berlin, Germany

## ABSTRACT

Recently, a volume penalization approach has been introduced that enables acoustic finite-difference time-domain (FDTD) simulations for complex geometries and supports the modeling of boundary impedances [1]. In this method, objects are modeled as porous materials by introducing an effective volume (porosity) and additional friction terms (flow resistance, permeability) into the governing equations. This contribution presents the approach in detail and investigates the numerical modeling error inherent in this methodology. The analysis focuses on rigid walls and reflections at these boundaries, exploring modeling with porosity, permeability, and their combination. The goal is to achieve a realistic approximation of the physical behavior by optimizing the choice of modeling parameters. This provides a deeper insight into the physics and functionality of the volume penalization approach and paves the way for further optimization possibilities.

**Keywords:** Numerical Acoustics, Finite Differences, Time Domain, Volume Penalization

## 1. INTRODUCTION

Time-domain methods enable the simulation of acoustic phenomena such as diffraction and variable sound propagation speeds, which are difficult to account for in geometrical acoustics [2]. Despite their high computational cost, increasing computing resources make them increasingly feasible for practical applications. The simulations are based on different sets of equations, including the wave equation, the nonlinear Euler equations, and their linearized form, the acoustic equations. Various numerical methods have been applied to solve these equations, such as finite difference, finite element, finite volume, and the discontinuous Galerkin method. A critical aspect of all these approaches is the implementation of boundary conditions, which significantly affects simulation accuracy [3]. Acoustic boundaries are often characterized by their impedance, a complex-valued quantity that is primarily used in frequency-domain analysis. Translating impedance models into the time domain remains challenging and is an active area of research.

A recent study introduced an immersed boundary method for time-domain simulations using finite differences [1], enabling impedance modeling. Immersed boundary methods enforce boundary conditions not directly on grid lines or element boundaries but rather through additional force-like terms in the governing equations. One such approach, the Brinkman volume penalization, represents objects as porous materials and has been widely applied in various fields, including aeroacoustics. The acoustic reflectivity of porous materials in the time domain has been analyzed in [4]. The volume penalization method presented in [1] employs a Brinkman-type approach that is physically motivated and capable of accurately representing both rigid walls and objects with typical acoustic impedances. It is straightforward to implement, computationally efficient, fully parallelizable, and does not require specialized grid adaptations near boundaries. The method is governed by two key parameters: a linear friction term $\chi$ (Darcy term), which accounts for fluid velocity (equivalent to particle velocity in a purely

**Corresponding author*: mathias.lemke@tnt.tu-berlin.de.

acoustic setting), and the effective volume fraction $\phi$, commonly referred to as porosity. Various formulations incorporating these parameters exist, as discussed in [5].

Although previous work has qualitatively and quantitatively demonstrated that the volume penalization approach [1] can effectively model solid walls and impedance boundary conditions, a rigorous analysis of the parameters $\phi$ and $\chi$ is still lacking. This study aims to provide such an analysis for the case of a solid wall. By systematically exploring different parameter combinations of $\phi$ and $\chi$, we evaluate the resulting error and determine the order of convergence with respect to spatial resolution.

## 2. GOVERNING EQUATIONS

The Euler equations are commonly used in acoustics as they describe both sound generation and propagation, including nonlinear effects. To introduce suitable impedance boundary conditions, the penalization is incorporated into the Euler equations using an effective volume $\phi$ [5] and a Darcy term proportional to $\chi$ [6].

$$\phi\partial_t(\rho) + \partial_{x_i}(\phi\rho u_i) = 0 \quad (1)$$
$$\phi\partial_t(\rho u_j) + \partial_{x_i}(\phi\rho u_i u_j) + \phi\partial_{x_j} p = \phi\chi(-u_j) \quad (2)$$
$$\phi\partial_t(\rho e_t) + \partial_{x_i}(\phi\rho u_i e_t + \phi u_i p) = 0 \quad (3)$$

Here, $\rho$ is the density, $u_j$ the velocity in the $x_j$-direction, $e_t$ the specific total energy, $p$ the pressure, and $\gamma$ the heat capacity ratio. For brevity, the dependency of variables on space and time is not explicitly stated. The summation convention applies for $i, j = [1, 2, 3]$. Assuming a constant heat capacity, the energy equation can be rewritten using [7]

$$e_t = (p/\rho) \cdot 1/(\gamma - 1) + (u_j u_j)/2, \quad (4)$$

leading to:

$$\phi\partial_t p + \gamma\partial_{x_i}(\phi u_i p) - (\gamma - 1)\phi u_i \partial_{x_i} p = 0. \quad (5)$$

### 2.1 Effective Volume ($\phi$)

The dimensionless effective volume $\phi$ represents the volume fraction $\phi(x_i) = V_{\text{fluid}}/V_{\text{total}}$ due to a porous medium, with values ranging between 0 and 1. For $\phi = 1$, the original Euler equations remain unchanged. For $\phi = 0$, the equations degenerate, which is avoided by choosing a small but finite value in simulations. Negative values or values greater than one are nonphysical and excluded. While time-dependent $\phi$ has been studied [5], it is not considered here. The presence of $\phi$ does not alter the local speed of sound and has minimal impact on the eigenvalues of the governing equations, allowing existing (aero-) acoustic solvers to be adapted with only minor modifications [5].

### 2.2 Darcy Term ($\phi\chi(-u_j)$)

The momentum equations include a penalization term $\phi\chi(-u_j)$, where $\chi(x_i)$ determines both the spatial distribution and the strength of the penalization. The parameter $\chi$ varies between 0 and $\infty$ and has units of Ns/m$^4$. For $\chi = 0$, the force term vanishes. Solid or semi-permeable boundaries can be represented using sufficiently large $\chi_s$ values [8]. However, increasing $\chi$ leads to larger negative eigenvalues of the right-hand-side operator, which in turn restricts the maximum allowable time step size and impacts the stability of standard time integration schemes. For acoustically damping porous materials modeled with the Darcy term, however, such restrictions typically do not arise.

### 2.3 Smoothing

To mitigate numerical issues such as stiffness [5], the values of the effective volume fraction $\phi(x_i)$ and permeability $\chi(x_i)$ are subjected to smoothing. In this work, a hyperbolic tangent function is employed for this purpose. For a wall located at $x_0$, the effective volume fraction is defined as:

$$\phi(x_i) = 1 - (1 - \phi_\epsilon)\frac{\tanh((x_i - x_0)/\delta_\phi) + 1}{2}, \quad (6)$$

where $\delta_\phi$ represents the smoothing width, and $\phi_\epsilon$ is the residual volume fraction within the wall. Similarly, the smoothing of the permeability is given by:

$$\chi(x_i) = \chi_\epsilon \frac{\tanh((x_i - x_0)/\delta_\chi) + 1}{2}, \quad (7)$$

where $\delta_\chi$ determines the smoothing width for permeability, and $\chi_\epsilon$ is the residual permeability at the wall. Alternative smoothing functions are also commonly employed, such as the error function (erf) or cosine masks, which may be preferable depending on the specific application, see [8]. However, it is the dominance of the parameters - particularly the amplitude and steepness - that plays a crucial role in shaping the acoustic behavior of the boundary. This sensitivity highlights the importance of choosing an appropriate smoothing function to accurately capture the physical effects at the boundaries.

## 3. NUMERICAL SETUP

To analyze the influence of the parameters and their interdependencies, a simple reflection at a flat wall is considered. The one-dimensional computational domain, spanning from $x = 0$ to $x = 3\,\mathrm{m}$, is discretized into equidistant points along the $x$-axis. The error is computed using $N_1 = 769$ points, and the convergence order is determined by calculating the error with a higher resolution of $N_2 = 1025$ points. An implicit, compact, 4th-order scheme is employed for the approximation of the spatial derivatives. The time integration is performed using a 4th-order Runge-Kutta scheme. The time step $\Delta t$ is chosen as $\Delta t = 7.9719 \times 10^{-6}\,\mathrm{s}$, corresponding to a CFL number of 0.7.

In addition to the volume penalization, the boundaries are assumed to be non-reflective and are implemented using characteristic boundary conditions. The initial condition is given by an adiabatic pressure pulse in front of the wall.

For evaluation, the following error is defined:

$$\text{error} = \int \frac{|p'_{\text{ref}} - p'_{\text{penalized}}|}{|p'_{\text{ref}}|} \mathrm{d}x \qquad (8)$$

Therein, $p'_{\text{ref}} = p_{\text{ref}} - p_\infty$ denotes the discretely exact solution of the reflection from a mirror source, while $p'_{\text{penalized}}$ denotes the solution resulting from volume penalization starting at the position $x = 1.5\,\mathrm{m}$.

## 4. RESULTS

Figure 1 shows the error as a function of the amplitudes of $\phi_\epsilon$ and $\chi_\epsilon$. The steepness parameter was set to $1.25\Delta x$ for both smoothing functions. As expected, the maximum error occurs at $\phi_\epsilon = 1$ and $\chi_\epsilon = 0$, which correspond to the absence of a wall. Furthermore, as physically expected, the error decreases with increasing permeability $\chi_\epsilon$, while the porosity remains constant at $\phi_\epsilon = 1$. If no permeability is modeled ($\chi_\epsilon = 0$), but the porosity ($\phi_\epsilon$) is reduced, the error also decreases. The minimum error is found with the smallest $\phi_\epsilon$ and no permeability. In this case, the method achieves the highest convergence order $\mathcal{O}(\Delta x^3)$, in contrast to using $\chi$ alone, where only $\mathcal{O}(\Delta x^{0.5})$ can be achieved. It should be noted that further increases in permeability, i.e. $\chi_\epsilon$, are possible, but they would require time integration methods that go beyond the stability properties of the classical 4th-order Runge-Kutta method, which is undesirable. The porosity, modeled by $\phi$, places significantly lower demands on the stability region of the time

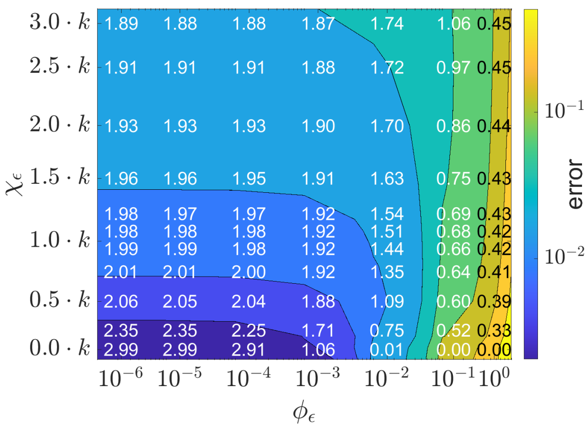


**Figure 1**. Visualization of the error (8) via the amplitudes of the porosity $\phi_\epsilon$ and permeability $\chi_\epsilon$ for a smoothing of $\delta_\phi$ and $\delta_\chi = 1.25\Delta x$. The white numbers correspond to the order of convergence of the error. The factor $k$ is defined as $k = \frac{\mathrm{s}}{\Delta t}\mathrm{Pa\,s\,m^{-2}}$.

integration, as discussed in [1]. Figure 2 shows the error as a function of the amplitude $\phi_\epsilon$ and the steepness parameter $\delta_\phi$. For large values of $\phi_\epsilon$, the smoothing parameter has almost no influence. For small values of $\phi_\epsilon$, the error decreases with decreasing $\delta_\phi$. The order of convergence is nearly unaffected by this. It should be noted that a too small $\delta_\phi$ for very small values of $\phi_\epsilon$ leads to instabilities, as evidenced by the missing areas in the figure. Figure 3 shows the error as a function of the amplitude $\chi_\epsilon$ and the steepness parameter $\delta_\chi$. As expected, the largest errors are found for small values of the permeability $\chi$. The error decreases for increasing values of $\chi_\epsilon$; with this effect being smaller for larger values of $\delta_\chi$. A maximum convergence order of 0.5 was achieved at the minimum error.

## 5. CONCLUSION

A volume penalization approach was presented, physically motivated by modeling boundaries as porous materials. The method is based on two key parameters: the effective volume fraction (porosity) $\phi$ and the Darcy term (permeability) $\chi$. An analysis was conducted to investigate the influence of these parameters by varying their amplitude and smoothing properties, comparing the results against a rigid wall test case. The findings indicate that porosity $\phi$ is significantly better suited for representing

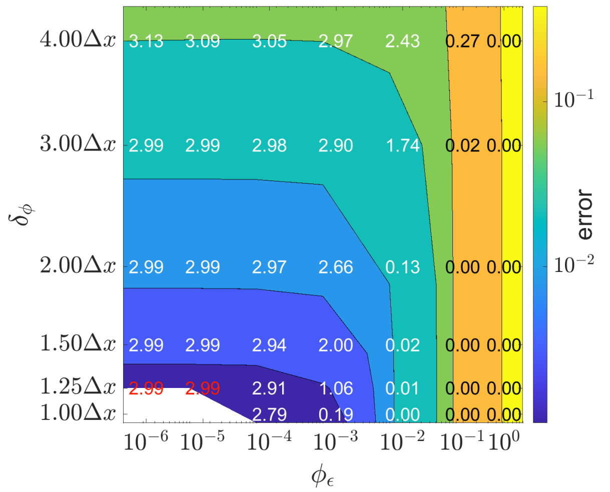


**Figure 2**. Mapping of the error as a function of $\phi_\epsilon$ and $\delta_\phi$. The white regions indicate parameter combinations that have led to an unstable simulation. The white/red numbers correspond to the order of convergence of the error.

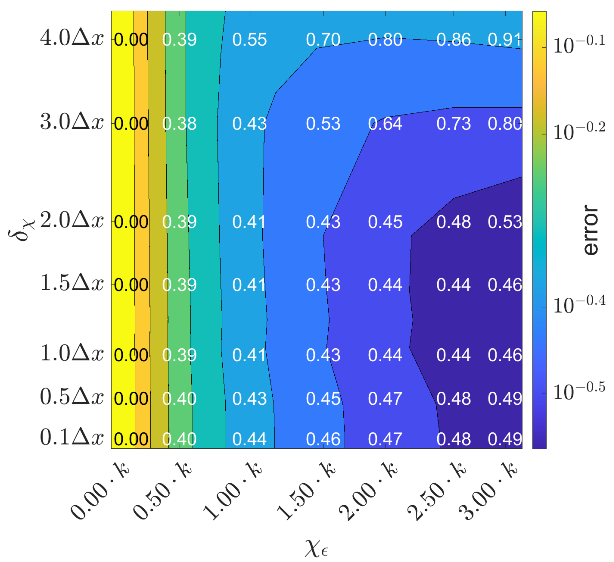


**Figure 3**. Visualization of the error as a function of $\chi_\epsilon$ and $\delta_\chi$. The white numbers correspond to the order of convergence of the error. The factor $k$ is defined as $k = \frac{\mathrm{s}}{\Delta t}\mathrm{Pa\,s\,m^{-2}}$.

acoustically hard walls, yielding lower errors and achieving a higher order of convergence. Additionally, $\phi$ imposes fewer constraints on time integration stability compared to permeability $\chi$. In general, the parameters must be chosen in accordance with their physical interpretation: porosity should be minimized where no air volume remains, and high permeability should only be applied with a sufficiently steep smoothing function. These insights offer valuable guidance for the appropriate selection of penalization parameters in future applications.

## 6. ACKNOWLEDGMENTS

The research was funded by the German Research Foundation - project number 504470212

## 7. REFERENCES


[1] M. Lemke and J. Reiss, “Approximate acoustic boundary conditions in the time-domain using volume penalization,” *The Journal of the Acoustical Society of America*, vol. 153, no. 2, pp. 1219–1228, 2023.

[2] M. Vorländer, *Auralization*. Springer, 2020.

[3] M. Vorländer, “Computer simulations in room acoustics: Concepts and uncertainties,” *The Journal of the Acoustical Society of America*, vol. 133, no. 3, pp. 1203–1213, 2013.

[4] D. K. Wilson, V. E. Ostashev, S. L. Collier, N. P. Symons, D. F. Aldridge, and D. H. Marlin, “Time-domain calculations of sound interactions with outdoor ground surfaces,” *Applied Acoustics*, vol. 68, no. 2, pp. 173–200, 2007.

[5] J. Reiss, “Pressure-tight and non-stiff volume penalization for compressible flows,” *Journal of Scientific Computing*, vol. 90, no. 3, pp. 1–29, 2022.

[6] R. Komatsu, W. Iwakami, and Y. Hattori, “Direct numerical simulation of aeroacoustic sound by volume penalization method,” *Computers & Fluids*, vol. 130, pp. 24 – 36, 2016.

[7] M. Lemke, J. Reiss, and J. Sesterhenn, “Adjoint based optimisation of reactive compressible flows,” *Combustion and Flame*, vol. 161, no. 10, pp. 2552 – 2564, 2014.

[8] M. Lemke, V. Citro, and F. Giannetti, “External acoustic control of the laminar vortex shedding past a bluff body,” *Fluid Dynamics Research*, vol. 53, p. 015506, feb 2021.